


# Biliverdin Reductase A Attenuates Hepatic Steatosis by Inhibition of Glycogen Synthase Kinase (GSK) 3 $\beta$ Phosphorylation of Serine 73 of Peroxisome Proliferator-activated Receptor (PPAR) $\alpha$ \*

Received for publication, April 13, 2016, and in revised form, September 30, 2016 Published, JBC Papers in Press, October 10, 2016, DOI 10.1074/jbc.M116.731703

 Terry D. Hinds, Jr.<sup>†1</sup>, Katherine A. Burns<sup>§¶1</sup>, Peter A. Hosick<sup>||\*\*</sup>, Lucien McBeth<sup>‡</sup>, Andrea Nestor-Kalinowski<sup>††</sup>, Heather A. Drummond<sup>||</sup>, Abdulhadi A. AlAmodi<sup>||</sup>, Michael W. Hankins<sup>||</sup>, John P. Vanden Heuvel<sup>§</sup>, and  David E. Stec<sup>||2</sup>

From the <sup>||</sup>Department of Physiology & Biophysics, Mississippi Center for Obesity Research, University of Mississippi Medical Center, Jackson, Mississippi 39216, the <sup>\*\*</sup>Department of Exercise Science and Physical Education, Montclair State University, Montclair, New Jersey 07043, the <sup>‡</sup>Center for Hypertension and Personalized Medicine, Department of Physiology & Pharmacology, <sup>††</sup>Advanced Microscopy & Imaging Center, Department of Surgery, University of Toledo College of Medicine and Life Sciences, Toledo Ohio 43614, the <sup>§</sup>Department of Veterinary and Biomedical Sciences, Pennsylvania State University, University Park, Pennsylvania 16802, and the <sup>¶</sup>Department of Environmental Health, Division of Environmental Genetics and Molecular Toxicology, University of Cincinnati College of Medicine, Cincinnati, Ohio 45267

Edited by Joel Gottesfeld

Non-alcoholic fatty liver disease is the most rapidly growing form of liver disease and if left untreated can result in non-alcoholic steatohepatitis, ultimately resulting in liver cirrhosis and failure. Biliverdin reductase A (BVRA) is a multifunctioning protein primarily responsible for the reduction of biliverdin to bilirubin. Also, BVRA functions as a kinase and transcription factor, regulating several cellular functions. We report here that liver BVRA protects against hepatic steatosis by inhibiting glycogen synthase kinase 3 $\beta$  (GSK3 $\beta$ ) by enhancing serine 9 phosphorylation, which inhibits its activity. We show that GSK3 $\beta$  phosphorylates serine 73 (Ser(P)<sup>73</sup>) of the peroxisome proliferator-activated receptor  $\alpha$  (PPAR $\alpha$ ), which in turn increased ubiquitination and protein turnover, as well as decreased activity. Interestingly, liver-specific BVRA KO mice had increased GSK3 $\beta$  activity and Ser(P)<sup>73</sup> of PPAR $\alpha$ , which resulted in decreased PPAR $\alpha$  protein and activity. Furthermore, the liver-specific BVRA KO mice exhibited increased plasma glucose and insulin levels and decreased glycogen storage, which may be due to the manifestation of hepatic steatosis observed in the mice.

These findings reveal a novel BVRA-GSK3 $\beta$ -PPAR $\alpha$  axis that regulates hepatic lipid metabolism and may provide unique targets for the treatment of non-alcoholic fatty liver disease.

Obesity is a worldwide epidemic that may be due to either genetic factors or by overeating and a sedentary lifestyle. During adipose tissue expansion, the number of adipocytes increase, as well as plasma glucose and fatty acid levels. During times of fasting, adipocytes release more fatty acids by lipolysis, which are shuffled to the liver and either produced into sugars from gluconeogenesis or stored as lipids (1). Long term obesity causes an overload of lipids in the liver, and fatty acid peroxidation, causing increased reactive oxygenase species and infiltration of immune cells. Non-alcoholic fatty liver disease (NAFLD)<sup>3</sup> is characterized by hepatic fat accumulation that, when coupled with another “hit,” such as increased oxidative stress, inflammation, or insulin resistance, can lead to the progression of non-alcoholic steatohepatitis (NASH) (2). However, hepatic steatosis may only represent the initial phase of several distinct injurious pathways rather than a true hit. Given this possibility, the initial “two-hit” theory for explaining the progression from NAFLD to NASH is now being modified to a “multiple parallel hits” hypothesis (3). In the multiple-hit model, the first hit is insulin resistance and associated metabolic disturbances, such as alterations in adipose tissue lipolysis increasing the efflux of free fatty acids from adipose to liver. The increase in free fatty acid delivery to the liver leads to hepatic

\* This work was supported by the University of Toledo deArce-Memorial Endowment Fund (T.D.H.). Research reported in this publication was also supported, in whole or part, by the National Institutes of Health [L32MD009154] (T.D.H.), the National Heart, Lung and Blood Institute [K01HL-125445] (T.D.H.) and [P01HL-051971], [HL088421] (D.E.S.), the National Institute of General Medical Sciences [P20GM-104357] (D.E.S.), the National Institute of Environmental Health Sciences [ES07799] (J.P.V.H.), and graduate student fellowship from Bristol Myers Squibb (K.A.B.). The authors declare that they have no conflicts of interest with the contents of this article. The content is solely the responsibility of the authors and does not necessarily represent the official views of the National Institutes of Health.

<sup>1</sup> To whom correspondence may be addressed: Dept. of Physiology and Pharmacology, 3000 Arlington Ave., Mailstop 1008, University of Toledo College of Medicine, Toledo, OH 43614. Tel.: 419-383-4465; Fax: 419-383-2871; E-mail: Terry.Hinds@utoledo.edu.

<sup>2</sup> To whom correspondence may be addressed: Dept. of Physiology & Biophysics, University of Mississippi Medical Center, 2500 North State St., Jackson, MS 39216. Tel.: 601-815-1859; Fax: 601-984-1817; E-mail: dstec@umc.edu.

<sup>3</sup> The abbreviations used are: NAFLD, non-alcoholic fatty liver disease; BVR, biliverdin reductase; GSK, glycogen synthase kinase; NASH, non-alcoholic steatohepatitis; PPAR, peroxisome proliferator-activated receptor; liver-specific BVRA knock-out; AMPK, AMP-activated protein kinase; FAS, fatty acid synthase; ACC, acetyl-CoA carboxylase; GYS, glycogen synthase; GTT, glucose tolerance test; ITT, insulin tolerance test; RIPA, radioimmune precipitation assay; MBP, maltose-binding protein; Tricine, N-[2-hydroxy-1,1-bis(hydroxymethyl)ethyl]glycine.

## Hepatic BVRA Reduces Steatosis by Inhibition of GSK3 $\beta$

steatosis, which causes the liver to be vulnerable to any hit that may follow, including increased oxidative stress and inflammation, thereby leading to hepatocyte injury and progression to NASH, liver fibrosis, cirrhosis, and ultimately liver failure. Factors that regulate insulin sensitivity, as well as reduce oxidative stress, minimize the capacity of immune signaling during hepatic lipid accumulation and prevent liver injury. We recently showed that induction of the heme oxygenase system and production of the antioxidant, bilirubin, reduced hepatic steatosis and lowered blood glucose (4).

The catabolism of heme from heme oxygenase produces biliverdin, which is reduced to bilirubin by biliverdin reductase (BVR), which exists as two isozymes: BVRA and BVRB (5). BVRB is the fetal isoform responsible for the production of bilirubin IX $\beta$  from biliverdin IX $\beta$  (6) and is only produced during the first 20 weeks after gestation. BVRB is expressed in adult tissues, but little is known about its function after fetal production of biliverdin IX $\beta$  has discontinued. The BVRA isoform is also expressed in adult tissues and is responsible for reducing biliverdin IX $\alpha$  to bilirubin IX $\alpha$ . In addition to functioning as a biliverdin reductase, BVRA can also function as a kinase and transcription factor and modulate insulin receptor signaling (5, 7). Despite the multiple functions of BVRA and bilirubin their roles, in protecting the liver from hepatic steatosis have yet to be established. We recently showed that BVRA-derived bilirubin IX $\alpha$  binds directly to the nuclear receptor transcription factor PPAR $\alpha$  to reduce adiposity and blood glucose (8). This is the first known ligand function reported for bilirubin. Importantly, PPAR $\alpha$  expression (4, 9, 10) and bilirubin levels are decreased in the obese (4, 9–11). The main function of PPAR $\alpha$  is to reduce hepatic steatosis through the burning of fatty acids via the regulation of genes involved in the  $\beta$ -oxidation pathway. The activation of PPAR $\alpha$  has been demonstrated to play a significant role in the attenuation of hepatic steatosis (14–16). PPAR $\alpha$  is a phosphoprotein; however, the regulation of the protein by phosphorylation by specific kinases and phosphatases are largely unknown (17). However, PPAR $\gamma$ , which induces fat storage in adipocytes and liver, has been shown to be regulated by kinases (18) and at least one phosphatase (19). Indeed, PPAR $\gamma$  induces hepatic steatosis (20). The mediation of lipid and glycogen storage in the liver is a delicate balance of kinase and phosphatase signaling during fasting and refeeding, as well as in lipid overload in fatty liver development. One of the major kinases involved in the progression of fatty liver is glycogen synthase kinase 3 $\beta$  (GSK3 $\beta$ ), which inhibits glycogen storage by the inhibition of glycogen synthase 2 via phosphorylation of the protein (21, 22). GSK3 $\beta$  activation plays a significant role in hepatic lipid accumulation and lipoapoptosis (23, 24). Regulation of GSK3 $\beta$  activity primarily occurs through phosphorylation at serine 9 of the protein, and increased phosphorylation of GSK3 $\beta$  at this residue decreases kinase activity.

In this study, we show *in vitro* and *in vivo* that hepatic BVRA can preserve PPAR $\alpha$  activity by increasing the phosphorylation of serine 9 in GSK3 $\beta$ . Furthermore, we show that GSK3 $\beta$  can increase phosphorylation of serine 73 in PPAR $\alpha$ , which causes rapid protein turnover and decreased overall PPAR $\alpha$  activity. Our data show a relationship between BVRA, GSK3 $\beta$ , and

PPAR $\alpha$  in the regulation of hepatic lipid metabolism and opens new avenues for therapeutic targeting.

### Results

*Liver-specific Deletion of BVRA Reduces Hepatic Insulin Signaling*—BVRA is an important protein regulating insulin signaling (5, 7, 25) and directly binds to and enhances phosphorylation of AKT (5) and ERK (26). The capacity of BVRA to regulate insulin signaling suggests a role in the management of diabetes; however, BVRA, to date, has not been studied in whole animals. We generated floxed BVRA mice and after crossing them to Alb-cre (B6.Cg-Tg(Alb-cre)21Mgn/J) mice, LBVRA-KO mice were developed (described in detail under “Experimental Procedures”). LBVRA-KO mice display decreased levels of BVRA mRNA and protein (Fig. 1, A–C), as well as significantly ( $p < 0.05$ ) less BVR activity in the liver (Fig. 1D). After LBVRA-KO mice were placed on a high fat diet, no differences in body weight, body composition, or plasma bilirubin levels were observed between the LBVRA-KO and flox control mice (Fig. 1, E–G). However, LBVRA-KO mice exhibited enhanced fasting hyperglycemia and hyperinsulinemia as compared with flox control mice (Fig. 1, H and I). Examination of insulin signaling pathways in the liver of LBVRA-KO found no differences in the levels of insulin receptor- $\beta$  (IR $\beta$ ) or the IR precursor (Fig. 2A). Interestingly, the levels of AKT phosphorylation (pAKT) were markedly decreased in LBVRA-KO livers compared with flox mice (Fig. 2B). LBVRA-KO mice exhibited an alteration in the glucose but not insulin tolerance test as compared with flox mice (Fig. 2, C and D). These results suggest that a liver-specific loss of BVRA promotes hepatic insulin resistance that, in turn, leads to increased plasma glucose and insulin levels, which most likely stemmed from reduced insulin signaling and not insulin receptor expression.

*BVRA Regulates Hepatic Lipid Accumulation*—The accumulation of lipids in the liver and the development of fatty liver lead to decreased hepatic insulin sensitivity, which affects whole body insulin turnover, thereby increasing systemic levels of insulin and glucose. High circulating insulin levels may also cause peripheral insulin resistance and glucose intolerance. Hepatic lipid accumulation in the LBVRA-KO and floxed mice was determined by Echo-MRI, hepatic triglyceride levels, and Oil Red O staining of tissues slices. Livers from LBVRA-KO mice had significantly ( $p < 0.05$ ) higher lipid levels compared with flox mice as shown by liver weight, hepatic triglycerides, and Oil Red O staining (Fig. 3, A–C). Several studies show increased phosphorylated AMP-activated protein kinase signaling is protective against hepatic steatosis. AMPK is activated by a decrease in ATP and a rise in cellular AMP (27–29), which lead to the phosphorylation of key enzymes that subsequently inhibit the synthesis of fatty acids and increase glucose uptake. Levels of phosphorylated AMPK were markedly decreased in LBVRA-KO mice compared with flox mice (Fig. 3D). Development of hepatic steatosis is linked to *de novo* production of fatty acids controlled by fatty acid synthase (FAS) and acetyl-CoA carboxylase (ACC). FAS is responsible for the production of long chain fatty acids that contribute to the triglyceride pool. Parallel with lipid accumulation, FAS was significantly increased in the liver of LBVRA-KO mice as compared with flox

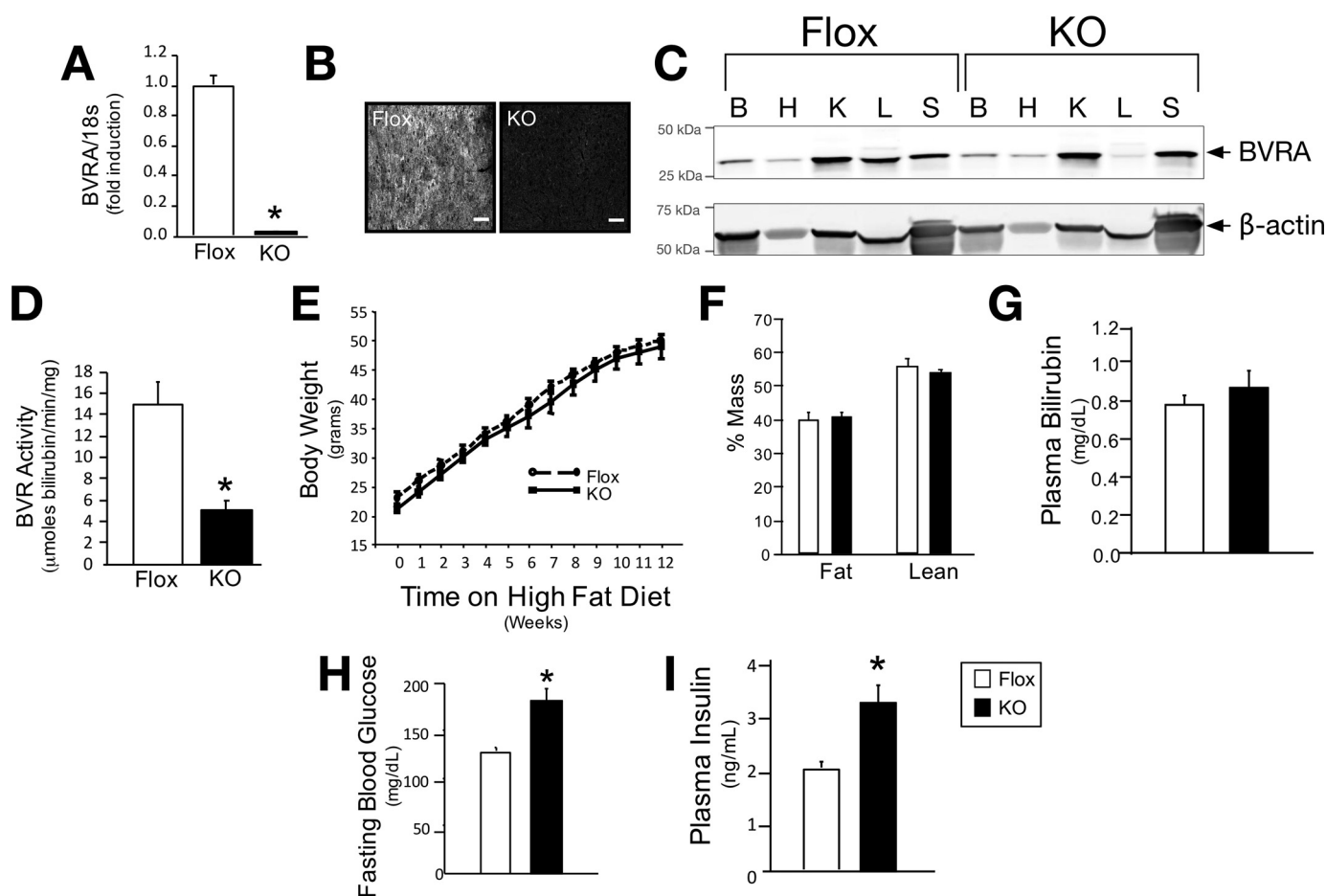


**FIGURE 1. Liver-specific knock-out of BVRA in mice increases blood glucose.** *A*, real time PCR of BVRA in the liver of LBVRA KO and flox mice. *B*, hepatic immunofluorescence staining for BVRA. Scale bars, 75  $\mu$ m. *C*, Western blot of BVRA from different tissues. *B*, brain; *H*, heart; *K*, kidney; *L*, liver; *S*, spleen. *D*, hepatic BVR activity. *E–I*, measurement of body weight (*E*), lean and fat mass (*F*), as well as plasma bilirubin (*G*), glucose (*H*), and insulin (*I*) in LBVRA KO and control flox mice. \*,  $p < 0.05$  (versus floxed mice;  $\pm$  S.E.;  $n = 6–8$ /group).

mice (Fig. 3*E*). Similarly, LBVRA-KO mice exhibited a significant reduction in the levels of phosphorylated ACC (Fig. 3*F*), which indicates enhanced ACC activity. ACC catalyzes the first steps of lipid synthesis involving the carboxylation of acetyl-CoA to malonyl-CoA. These data demonstrate that the loss of hepatic BVRA resulted in an enhancement of proteins and signaling pathways involved in the synthesis of fatty acids, which contributed to hepatic steatosis.

**BVRA Regulates GSK3 $\beta$  and Hepatic Glycogen Storage**—Glycogen synthase is the key enzyme involved in the storage of glucose as glycogen in liver and muscle. Glycogen synthase 2 (GYS2) is the predominant isoform found in the liver that is responsible for glycogen production. Phosphorylation at serine 641 by GSK3 $\beta$  inhibits activity of GYS2 and causes decreased glycogen storage (21, 22). Conversely, for glycogen storage, GSK3 $\beta$  is inhibited by phosphorylation of serine 9. GSK3 $\beta$  phosphorylation was measured by two methods: Western blotting and a phosphoserine 9 GSK3 $\beta$ -specific ELISA. The levels of serine 9 phosphorylated GSK3 $\beta$  were significantly decreased in the liver of LBVRA-KO as compared with flox control mice (Fig. 4*A*), which indicates activation. The increased GSK3 $\beta$  activity in LBVRA-KO mice is supported by decreased liver glycogen stores, GYS2 mRNA, and increased levels of phosphorylated GYS2 when compared with flox mice (Fig. 4, *B–D*).

These data demonstrate that BVRA decreases GSK3 $\beta$  activity to enhance glycogen storage.

**BVRA Regulates PPAR $\alpha$  Expression and Activity in the Liver**—Hepatic steatosis arises from increased synthesis of fatty acids or by decreasing the burning of fat ( $\beta$ -oxidation). PPAR $\alpha$  also binds to the promoter of GYS2 to increase expression (30), which together interacts to regulate glycogen storage and steatosis. PPAR $\alpha$  regulation of lipid accumulation derives mainly from carnitine palmitoyltransferase-1A (CPT1A) and fibroblast growth factor 21 (FGF21). CPT1A is the rate-limiting enzyme in mitochondrial fatty acid  $\beta$ -oxidation. PPAR $\alpha$ , and regulated gene CPT1A, protein levels were significantly ( $p < 0.05$ ) decreased in the liver of LBVRA-KO as compared with flox mice (Fig. 5, *A* and *B*). The reduction in PPAR $\alpha$  activity was confirmed by examining the expression of several of its target genes in the liver (Fig. 5, *B* and *C*). FGF21, a major PPAR $\alpha$  target gene whose hepatic expression and plasma levels were also significantly decreased in LBVRA-KO as compared with flox mice (Fig. 5*D*). These data show that BVRA is a major regulator of  $\beta$ -oxidation by mediating PPAR $\alpha$  expression and activity.

**GSK3 $\beta$  Regulates PPAR $\alpha$  Activity Predominately through Phosphorylation of Serine 73**—To determine the effect of GSK3 $\beta$  on PPAR $\alpha$  expression and activity, we examined a



## Hepatic BVRA Reduces Steatosis by Inhibition of GSK3 $\beta$

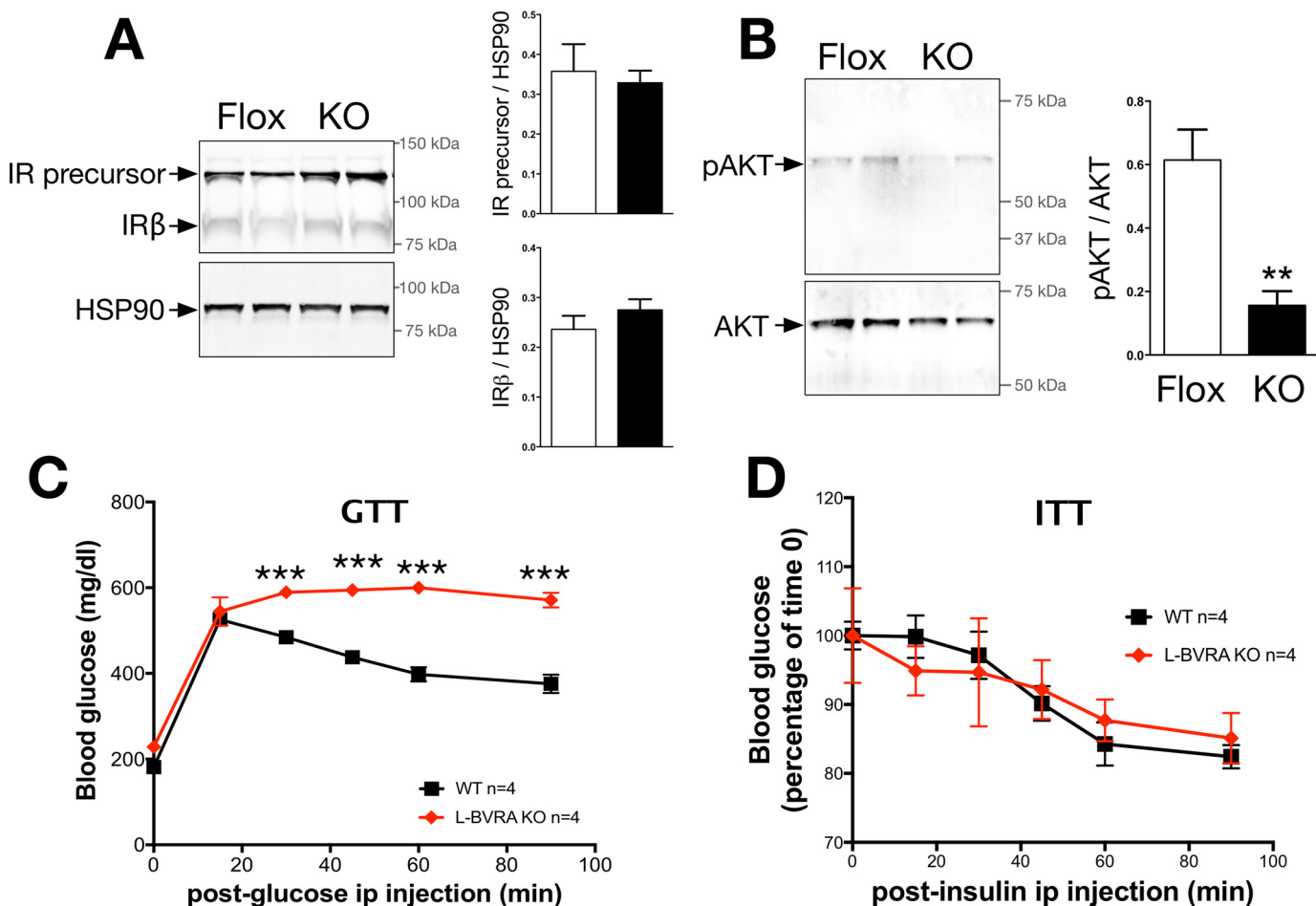
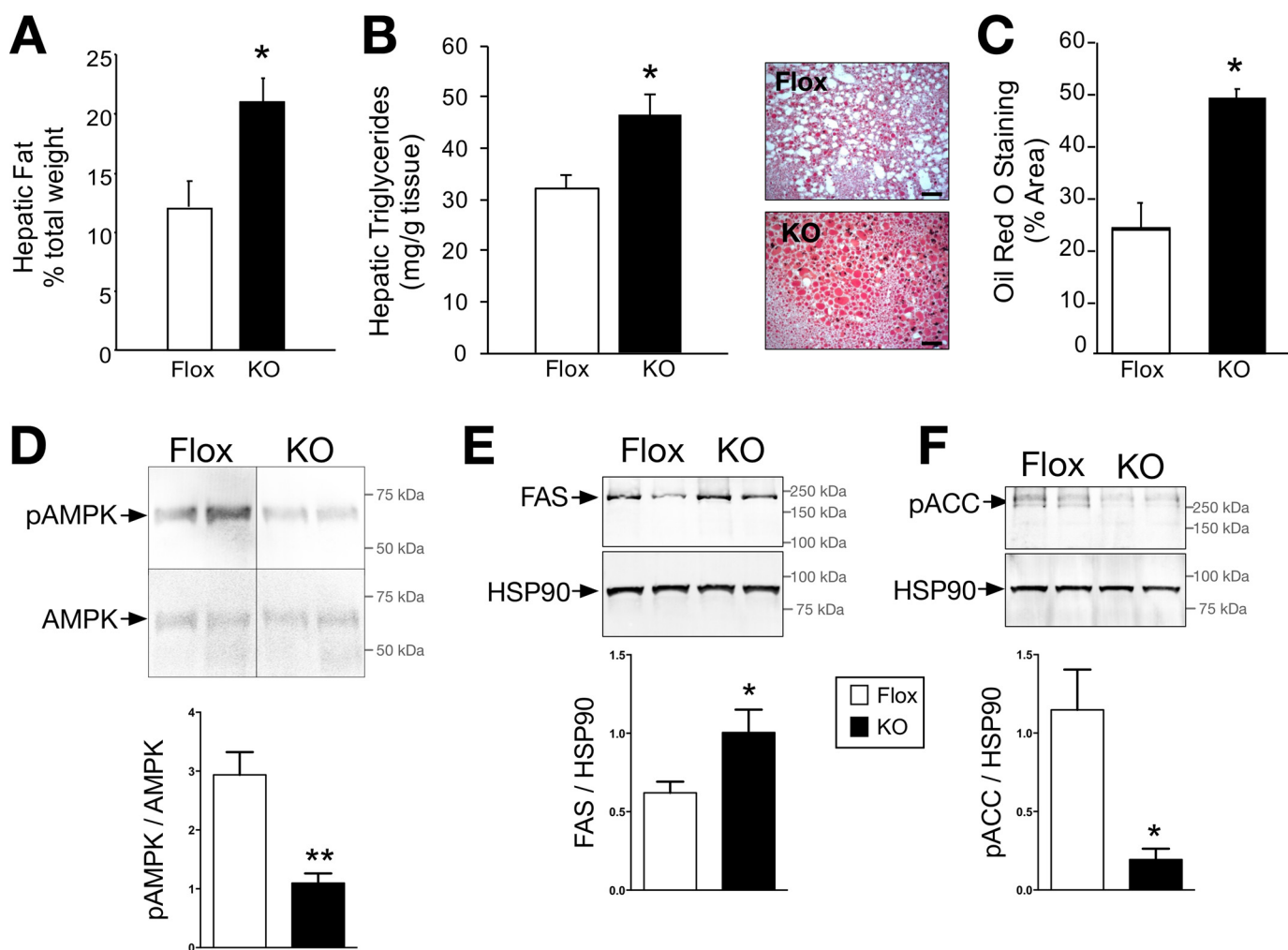


FIGURE 2. **BVRA regulates hepatic insulin signaling.** *A* and *B*, Western blot and densitometry of the insulin receptor precursor and insulin receptor- $\beta$  (IR $\beta$ ) in the liver (*A*) or AKT1/2 and phosphorylated AKT in the liver (*B*). *C*, GTT. *D*, ITT in L-BVRA KO and control flox mice. \*\*,  $p < 0.01$  (versus flox mice;  $\pm$  S.E.;  $n = 4$ ); \*\*\*,  $p < 0.001$  (versus flox mice;  $\pm$  S.E.;  $n = 4$ ).

series of experiments utilizing kinase assays, ubiquitination, and the minimal PPRE-3tk-Luc construct. PPAR $\alpha$  has four major structural domains, the A/B (activation factor), C (DNA binding domain), D, and E/F (ligand binding) domains, that harbor five potential GSK3 phosphorylation sites (serines 59, 73, 76, 89, and 163) that are conserved across mammalian species (Fig. 6A). *In vitro* kinase assays showed that GSK3 $\beta$ , based on kinase level, directly phosphorylates PPAR $\alpha$  (Fig. 6B). To localize the sites within PPAR $\alpha$  directly phosphorylated by GSK3 $\beta$ , *in vitro* kinase assays were performed with purified PPAR $\alpha$  domain proteins (Fig. 6C). Full-length PPAR $\alpha$  was a substrate for phosphorylation by GSK3 $\beta$ ; however, the A/B domain of PPAR $\alpha$  was a better substrate for GSK3 $\beta$  phosphorylation in this assay (Fig. 6C). No phosphorylation occurred in the C-domain, despite the fact that it contains a consensus GSK3 binding site. Furthermore, no phosphorylation was observed in the D and E/F domains of the PPAR $\alpha$  protein. Mutational analysis of serine S59A, S73A, S76A, and S89A in the PPAR $\alpha$  protein revealed that serine 73 (Ser<sup>73</sup>) was the primary site in the A/B domain phosphorylated by GSK3 $\beta$  (data not shown). To determine whether GSK3 $\beta$  mediates ubiquitination of PPAR $\alpha$  protein by increasing Ser<sup>73</sup> phosphorylation, we performed transfections with WT PPAR $\alpha$  or S73A PPAR $\alpha$  in the presence of GSK3 $\beta$ , ubiquitin, or empty vector. The cells

were treated with DMSO or WY-14643 in the presence of MG132, a proteasome inhibitor. The co-expression of PPAR $\alpha$  and GSK3 $\beta$  dramatically increased the ubiquitination of PPAR $\alpha$  relative to receptor alone (Fig. 6D). A ligand-dependent increase in ubiquitination was observed with receptor alone (*fifth* and *sixth* lanes), but no appreciable difference in ligand-dependent ubiquitination was observed with the overexpression of GSK3 $\beta$  (*seventh* and *eighth* lanes). The overexpression of GSK3 $\beta$  with S73A PPAR $\alpha$  resulted in increased ubiquitination (*tenth* and *eleventh* lanes), but decreased ubiquitination of S73A PPAR $\alpha$  was seen relative to WT receptor (*twelfth* and *thirteenth* lanes) (Fig. 6D). To determine whether GSK3 $\beta$  mediates PPAR $\alpha$  activity, we overexpressed GSK3 $\beta$  in a concentration-dependent manner and measured PPAR $\alpha$ -dependent activation of the minimal PPRE promoter luciferase activity (PPRE-3tk-luc). Increasing concentrations of GSK3 $\beta$  decreased PPAR $\alpha$  activation with ligand, which was not observed in the empty vector control (Fig. 6E). However, a K85A kinase-dead mutation of GSK3 $\beta$  failed to attenuate PPAR $\alpha$ -dependent activation of the PPRE promoter luciferase activity (Fig. 6F). Altogether, these data demonstrate that GSK3 $\beta$  affects the ubiquitination of PPAR $\alpha$  by increasing phosphorylation of Ser<sup>73</sup> in PPAR $\alpha$ , which ultimately inhibits activity.



**FIGURE 3. The loss of hepatic BVRA causes lipid accumulation.** A, hepatic fat measured by Echo-MRI. B, biochemical measurement of hepatic triglyceride levels. C, Oil Red O staining of liver sections and densitometry. Scale bars, 50  $\mu$ m. D–F, representative Western blot of hepatic expression of AMPK and phosphorylated AMPK (D), FAS (E), and phosphorylated ACC (F). \*,  $p < 0.05$ ; \*\*,  $p < 0.01$  (versus flox mice;  $\pm$  S.E.;  $n = 4$ ).

*LBVRAKO Mice Have Decreased PPAR $\alpha$  Expression and Enhanced Serine 73 Phosphorylation in the Liver*—To determine the role of serine 73 phosphorylation on PPAR $\alpha$  activity, we examined S73A PPAR $\alpha$ , which should be resistant to GSK3 $\beta$ -mediated phosphorylation. In addition, a serine to aspartic acid S73D PPAR $\alpha$  mutation was created to mimic constitutive GSK3 $\beta$ -mediated phosphorylation. S73A PPAR $\alpha$  had significantly ( $p < 0.01$ ) higher basal activity as compared with WT PPAR $\alpha$  (Fig. 7A). However, no difference was observed with WY-14643-induced PPAR $\alpha$  activity. In contrast, S73D PPAR $\alpha$ , that mimics hyperphosphorylation by GSK3 $\beta$  resulted in decreased basal and WY-14643-mediated activation of PPAR $\alpha$  activity (Fig. 7A). To detect serine 73 phosphorylation of PPAR $\alpha$ , a rabbit phospho-specific antibody (Ser(P)<sup>73</sup> PPAR $\alpha$ -Ab) was generated. Specificity of Ser(P)<sup>73</sup> PPAR $\alpha$ -Ab was determined by transfecting COS-7 cells with FLAG-tagged PPAR $\alpha$ , followed by immunostaining with Ser(P)<sup>73</sup> PPAR $\alpha$ -Ab and FLAG antibodies. As predicted, Ser(P)<sup>73</sup> PPAR $\alpha$ -Ab detected PPAR $\alpha$  WT but showed no reactivity when blocked with the Ser(P)<sup>73</sup> peptide used to create the antibody (Fig. 7B). Levels of phosphorylated serine 73 were determined in the liver of LBVRA-KO and flox mice using the Ser(P)<sup>73</sup> PPAR $\alpha$  specific

antibody. The ratio of phosphorylated serine 73 to total PPAR $\alpha$  immunostaining significantly ( $p < 0.01$ ) increased in LBVRA-KO mice as compared with flox mice (Fig. 7C). The increase in phosphorylated Ser<sup>73</sup> PPAR $\alpha$  is consistent with decreased phosphorylation of Ser<sup>9</sup> GSK3 $\beta$  in the liver of LBVRA-KO mice. These data also demonstrate, for the first time, that BVRA regulates GSK3 $\beta$ -mediated phosphorylation of PPAR $\alpha$ , which significantly contributes to the control of hepatic lipid metabolism.

## Discussion

We report here, for the first time, a new hepatic signaling paradigm for BVRA, which regulates steatosis by inhibition of GSK3 $\beta$  and activation of PPAR $\alpha$ . There is insufficient knowledge of the role of BVRA in the regulation of hepatic lipid accumulation or in insulin signaling. However, the interaction between BVRA and AKT has been previously reported. The Maines laboratory (25) demonstrated BVRA mediates insulin signaling and glucose uptake in human skeletal muscle cells. Other studies indicate suppression of BVRA by siRNA decreased pAKT in HK-2 proximal tubule epithelial human cells (31) and rat heart H9c2 cells (32), suggesting that BVRA

## Hepatic BVRA Reduces Steatosis by Inhibition of GSK3 $\beta$

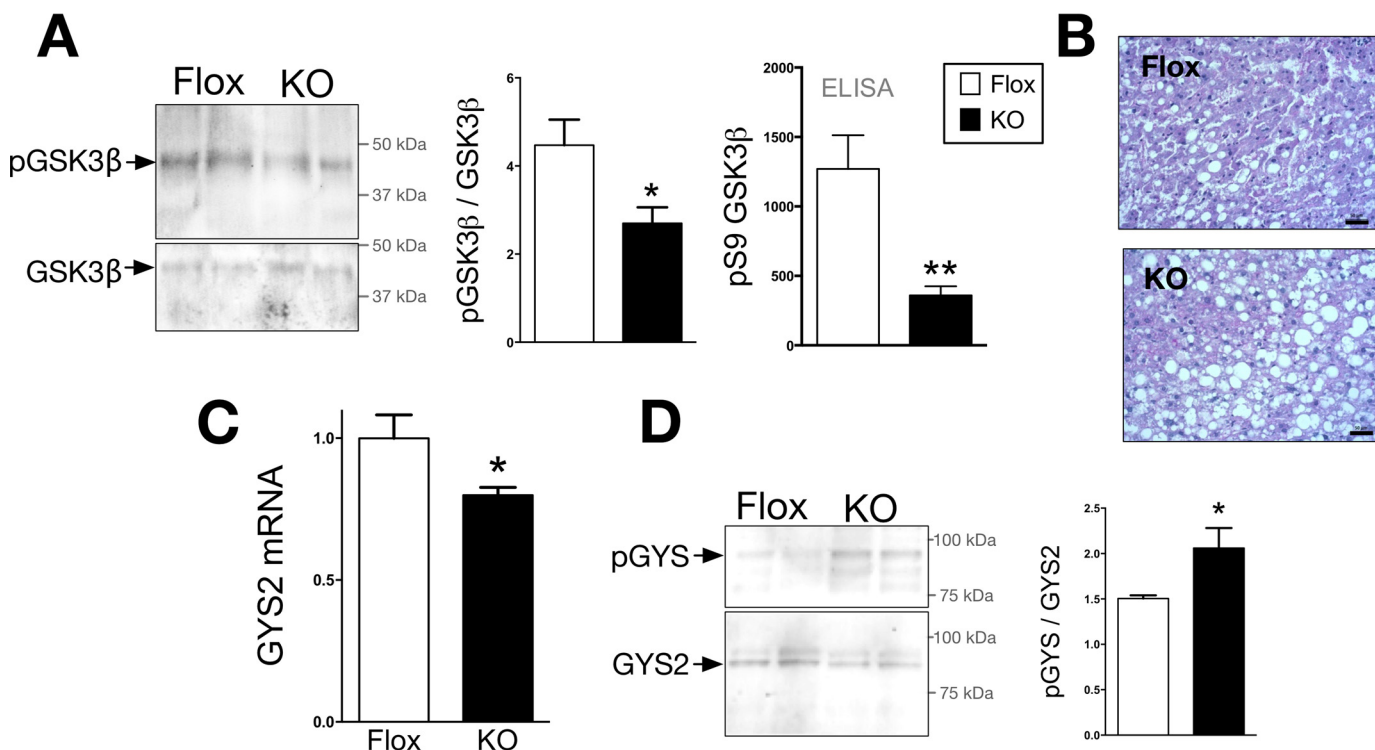


FIGURE 4. **GSK3 $\beta$  is more active in the LBVRA KO mice and suppresses glycogen storage.** A and B, Western blot and densitometry of hepatic total and phosphorylated GSK3 $\beta$  and levels of serine 9 phosphorylated (pS9) GSK3 $\beta$  measured by ELISA (A) and periodic acid Schiff staining for glycogen in liver (B). Scale bars, 50  $\mu$ m. C, real time PCR measurement of hepatic expression levels of GYS2 mRNA. D, representative Western blot of hepatic GYS2 and serine 641 phosphorylation of GYS. \*,  $p < 0.05$ ; \*\*,  $p < 0.01$  (versus flox mice;  $\pm$  S.E.;  $n = 4$ ).

may positively affect glucose uptake. In this study, we show that the LBVRA-KO mice had significantly reduced phosphorylation of AKT in the liver and higher plasma glucose and insulin levels. LBVRA-KO mice also exhibited alterations in glucose tolerance tests (GTTs) but not insulin tolerance tests (ITTs), suggesting alterations in hepatic insulin sensitivity. Interestingly, the body weight, fat and lean mass, and plasma bilirubin levels were the same as observed in the floxed mice. However, the LBVRA-KO mice had more lipids in the liver. Lipid accumulation in the liver leads to hepatic insulin resistance that can manifest into peripheral insulin resistance and eventually non-insulin dependent type II diabetes mellitus. The increased expression of FAS and phosphorylated ACC in the LBVRA-KO mice, which are involved in fatty acid synthesis, correlates with the development of hepatic steatosis in response to high fat diet feeding. FAS can generate lipids that can act as intracellular signaling molecules that are capable of regulating genes involved in the oxidation of fatty acids and fat storage. ACC is the rate-limiting enzyme that catalyzes lipids for synthesis involving the carboxylation of acetyl-CoA to malonyl-CoA, which is then used for the storage of fat. ACC activity is inhibited via phosphorylation by AMPK, which, along with PPAR $\alpha$ , increases the burning of fat through the  $\beta$ -oxidation pathway. The phosphorylation of ACC and AMPK was significantly reduced in LBVRA KO mice, indicating reduced burning of fat through  $\beta$ -oxidation. PPAR $\alpha$  increases key regulators of  $\beta$ -oxidation, CPT1 and FGF21, which CPT1 binds to long chain fatty acids in the mitochondria for lipid metabolism. FGF21 is a hepatic hormone that decreases fat in liver and increases glucose uptake (4, 33–36). Indeed, the LBVRA-KO mice exhibited

reduced levels of hepatic CPT1A and FGF21. Other PPAR $\alpha$  target genes GYS2, CD36, G6Pase, glucokinase, CYP2J6, and CYP4A12 were significantly reduced in the livers of the LBVRA-KO mice. Overall, the loss of hepatic BVRA resulted in a decrease in the pathway for fatty acid oxidation and glycogen storage, as well as an increase in fatty acid synthesis and marked hepatic steatosis that most likely contributed to the increased blood glucose and insulin levels.

Our study identifies a novel pathway by which BVRA can regulate hepatic PPAR $\alpha$  levels through the modulation of GSK3 $\beta$ -mediated phosphorylation of Ser(P)<sup>73</sup>. BVRA has been recently shown to directly interact with GSK3 $\beta$  (37). Our data demonstrate that BVRA prevents GSK3 $\beta$  phosphorylation of PPAR $\alpha$  at serine 73 to decrease ubiquitin-mediated degradation of the protein. GSK3 $\beta$  is implicated in fatty liver disease and apoptosis, and small molecule inhibitors of GSK3 $\beta$  are demonstrated to protect against obesity-induced hepatic steatosis (38–41). LBVRA-KO mice have lower GSK3 $\beta$  phosphorylation, which is indicative of kinase activation (21, 42). GSK3 $\beta$  activation was also evident by the enhanced phosphorylation of GYS2 in the liver of LBVRA-KO mice. Interestingly, the LBVRA-KO mice also had enhanced phosphorylation of serine 73 in PPAR $\alpha$ , as well as decreased PPAR $\alpha$  expression and activity. We show that the decline in PPAR $\alpha$  activity and expression was mediated by GSK3 $\beta$ , which was most likely to reduce  $\beta$ -oxidation and glycogen storage pathways. The importance of Ser(P)<sup>73</sup> in PPAR $\alpha$  regulation is further established by our findings that a mutation of this serine residue to an alanine is resistant to GSK3 $\beta$ -mediated phosphorylation and decreased the activity of the protein. In contrast, mutation of this residue to

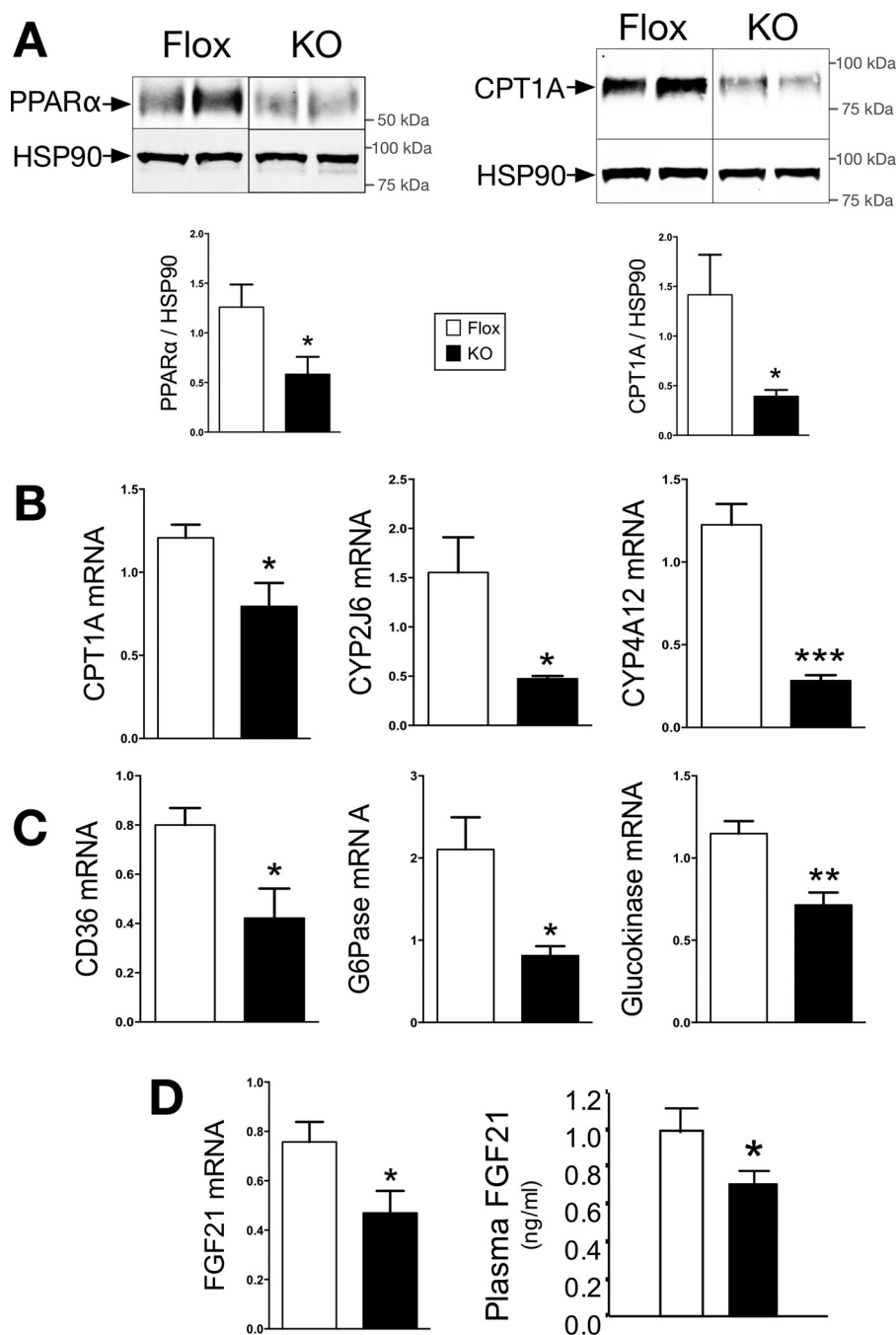


FIGURE 5. **PPAR $\alpha$  expression and activity are reduced in LBVRA KO mice.** *A* and *B*, Western blot and densitometry of hepatic protein levels of CPT1A and PPAR $\alpha$  (*A*), and real time PCR of CPT1A, CYP2J6, and CYP4A12 mRNA (*B*). *C*, real time PCR of CD36, G6Pase, and glucokinase mRNA. *D*, real time PCR of FGF21 mRNA and plasma FGF21 level in LBVRA KO and control flox mice. \*,  $p < 0.05$  (versus flox mice;  $\pm$  S.E.;  $n = 4$ ).

aspartic acid to mimic GSK3 $\beta$ -mediated phosphorylation resulted in decreased PPAR $\alpha$  activity under basal conditions and response to WY-14643 treatment. Taken together, these data identify Ser(P)<sup>73</sup> of PPAR $\alpha$  as a GSK3 $\beta$  target that is inhibited by hepatic BVRA to regulate fatty acid metabolism in liver and enhance PPAR $\alpha$ -mediated gene transcription of the  $\beta$ -oxidation pathway (Fig. 8).

Although we have identified a novel pathway by which BVRA can decrease hepatic steatosis via inhibition of GSK3 $\beta$  mediated phosphorylation of PPAR $\alpha$ , this pathway may also impact lipid accumulation through the intracellular production of bil-

irubin. Bilirubin is a powerful antioxidant molecule (43, 44). In addition to being a potent antioxidant, bilirubin has anti-inflammatory properties and can serve to prevent other types of cell stressors, such as endoplasmic reticulum stress (25–27). Several studies demonstrate increased serum bilirubin levels are associated with decreased hepatic steatosis (45–47). Despite these correlative studies, which show a protective effect of serum bilirubin on hepatic steatosis, the mechanism by which bilirubin offers this safeguard is not currently known. However, we recently identified bilirubin as a novel PPAR $\alpha$  agonist (8). Interestingly, its precursor, biliverdin, does not bind



## Hepatic BVRA Reduces Steatosis by Inhibition of GSK3 $\beta$

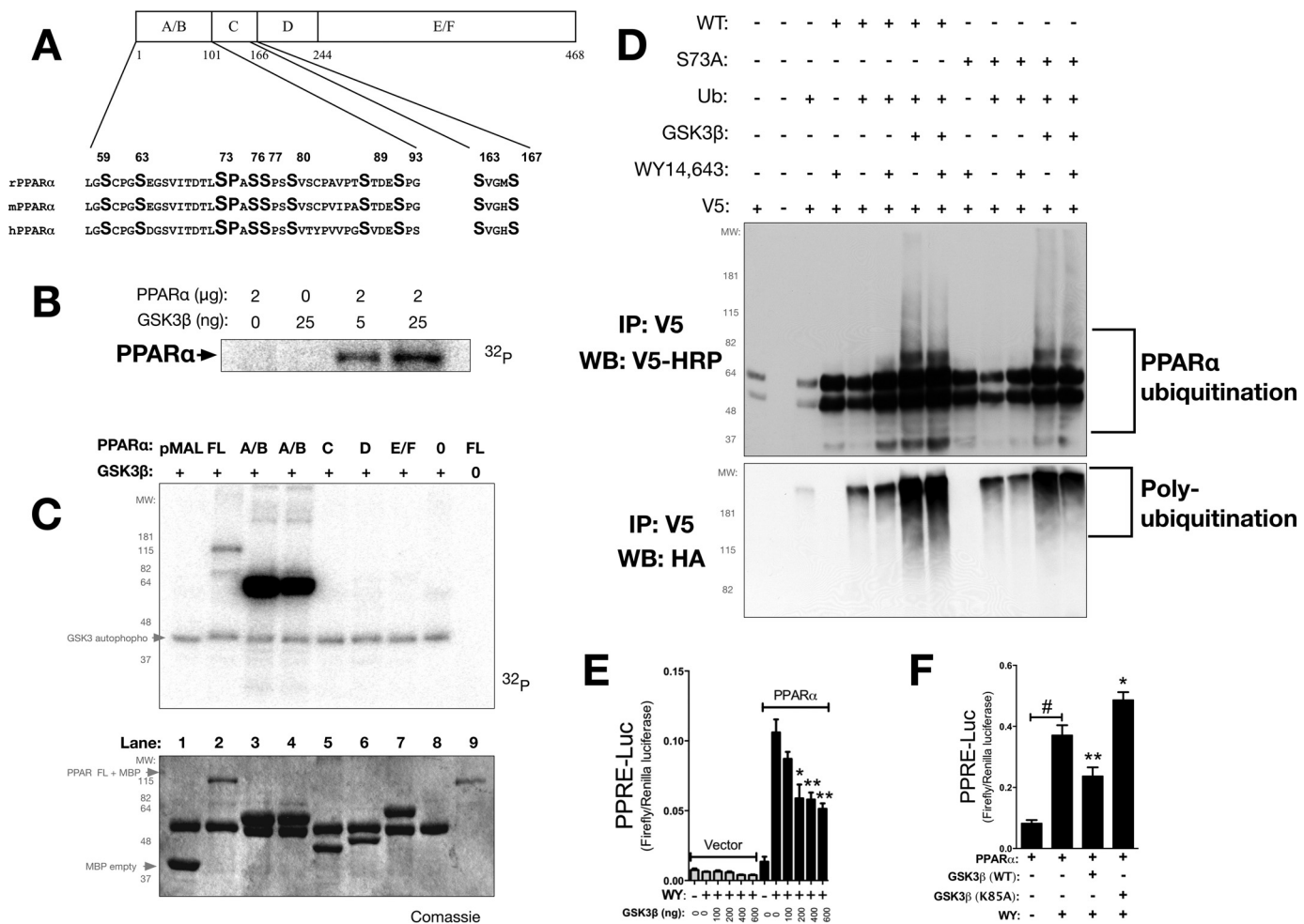


**FIGURE 6. GSK3 $\beta$  targets PPAR $\alpha$  by phosphorylation at serine 73 for degradation.** *A*, graphical representation of serines in the activation factor-1 A/B domains of rat (*rPPAR $\alpha$* ), mouse (*mPPAR $\alpha$* ), and human (*hPPAR $\alpha$* ). PPAR $\alpha$  contains five putative GSK3 consensus phosphorylation sites within the A/B and C domains. *B*, purified bacterially expressed pMAL-PPAR $\alpha$  wild-type was incubated with [ $\gamma$ - $^{32}$ P]ATP in the presence of increasing amounts of activated GSK3 $\beta$ . *C*, purified bacterially expressed pMAL-PPAR $\alpha$  full-length (FL) and domains (A/B, C, D, and E/F) were incubated with [ $\gamma$ - $^{32}$ P]ATP in the presence (+) or absence (-) of activated GSK3 $\beta$  (top panel). A Coomassie stain of the *in vitro* kinase assay was performed (bottom panel; representative of three or more experiments). *D*, Cos-1 cells were transfected with an HA-tagged ubiquitin expression vector, V5-rPPAR $\alpha$ , V5-PPAR $\alpha$  S73A, and/or pcDNA GSK3 $\beta$ . The cells were co-treated with vehicle or 50  $\mu$ M WY-14643 and 5  $\mu$ M MG132 for 4 h. PPAR $\alpha$  protein was immunoprecipitated (IP) and analyzed by Western blotting (WB) using anti-V5 and anti-HA antibodies (representative of three experiments). *E*, PPAR $\alpha$  activity at the minimal promoter PPRE-3tk-luc with increasing doses of GSK3 $\beta$  (0, 100, 200, 400, and 600 ng) with empty vector (100 ng) or PPAR $\alpha$  (100 ng) in the presence of vehicle (WY -) or WY-14643 (WY +). \*,  $p < 0.05$ ; \*\*,  $p < 0.01$  (versus WY -, 0 GSK3 $\beta$ , PPAR $\alpha$  control;  $\pm$  S.E.;  $n = 4$ ). PPAR $\alpha$  and GSK3 $\beta$  WT and K85A mutant with the minimal promoter PPRE-3tk-luc were transfected in Cos-7 and treated with WY-14643 or vehicle for 24 h. *F*, PPAR $\alpha$  activity at the minimal promoter PPRE-3tk-luc with WT GSK3 $\beta$  or kinase-dead K85A GSK3 $\beta$  in the presences of vehicle (WY -) or WY-14643 (WY +). \*,  $p < 0.05$ ; \*\*,  $p < 0.01$  (versus WY +, - GSK3 $\beta$ , + PPAR $\alpha$ ;  $\pm$  S.E.;  $n = 4$ ).

PPAR $\alpha$  efficiently (8). Acute treatment of mice with bilirubin resulted in an increased hepatic PPAR $\alpha$  target genes, including FGF21, which was not observed in the liver or plasma of PPAR $\alpha$  knock-out mice (8). Our results here demonstrate that hepatocyte-specific deletion of BVRA decreases PPAR $\alpha$  activity in the liver through alterations in GSK3 $\beta$  activity; however, the loss of bilirubin-derived PPAR $\alpha$  signaling increased hepatic steatosis in mice fed a high fat diet cannot be ruled out. However, BVRA has a 2-fold protection mechanism against NAFLD and fatty liver disease: 1) production of bilirubin that functions as an antioxidant and PPAR $\alpha$  ligand and 2) BVRA activation of AKT and inhibition of GSK3 $\beta$  (Fig. 8). The degree to which the loss of bilirubin production contributes to this phenotype will need to be examined in future studies.

In conclusion, NAFLD, caused by the high rate of obesity, is the most rapidly growing form of liver disease in the general

population. Currently, there are no effective treatments for NAFLD, and if combined with an additional hit to the liver, it can progress to NASH and ultimately liver failure. We have identified a novel pathway by which BVRA regulates hepatic steatosis by regulating GSK3 $\beta$ -mediated phosphorylation of Ser(P)<sup>73</sup> of PPAR $\alpha$ , which increases protein degradation and loss of PPAR $\alpha$  signaling. Our results suggest that hepatic BVRA or BVRA-mediated bilirubin will increase the burning of fat and sensitization to insulin and glucose intolerance. The BVRA-AKT-PPAR $\alpha$  axis is a major signaling paradigm, preventing fatty liver disease and insulin resistance.

### Experimental Procedures

**Animals**—The experimental procedures and protocols of this study conform to the National Institutes of Health Guide for the Care and Use of Laboratory Animals and were approved



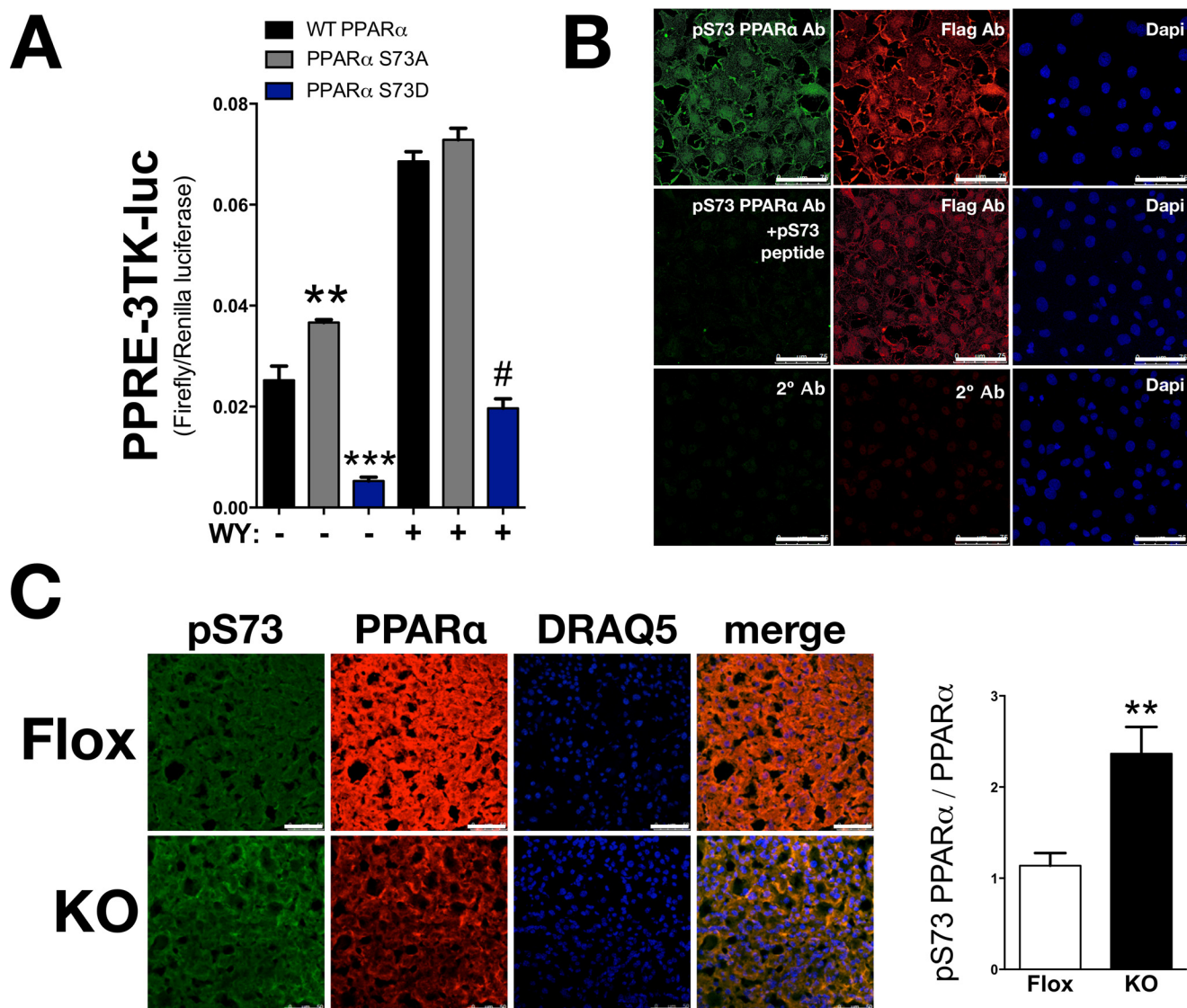


FIGURE 7. PPAR $\alpha$  serine 73 phosphorylation is increased in LBVRA KO mice. *A*, PPAR $\alpha$  WT, S73A, and S73D mutants with the minimal promoter PPRE-3tk-luc were transfected in Cos-7 and treated with WY-14643 or vehicle for 24 h. *B*, COS-7 cells were transfected with a FLAG-tagged PPAR $\alpha$  construct for 24 h followed by immunostaining with antibodies to Ser(P)<sup>73</sup> PPAR $\alpha$ -Ab or FLAG or with Ser(P)<sup>73</sup> PPAR $\alpha$ -Ab plus blocking peptide used to construct the antibody, as well as negative control with only secondary antibodies. Scale bars, 75  $\mu$ m. *C*, levels of phosphorylated serine 73 (green), total PPAR $\alpha$  (red), and nuclear staining (blue) with DRAQ5 in the liver of LBVRA KO and flox mice. Scale bars, 50  $\mu$ m. \*\*,  $p < 0.01$  (versus floxed mice;  $\pm$  S.E.;  $n = 4$ ).

by the Institutional Animal Care and Use Committee of the University of Mississippi Medical Center in accordance with the NIH Guide for the Care and Use of Laboratory Animals. All mice had free access to food and water *ad libitum*. Animal activity and grooming were monitored daily to assess overall animal health. The animals were housed in a temperature-controlled environment with 12 h dark-light cycle. BVRA conditional knock-out mice were generated from gene targeted embryonic stem cells purchased from the European Conditional Mouse Mutagenesis Program (EUCOMM, clone HEPD0510\_3\_B01) and injected into blastocysts. The stem cells contained an altered copy of the BVRA gene, in which exon 2 was flanked by loxP sites. The neomycin/lacZ cassette was then removed by breeding to Flp (B6.Cg-Tg(Pgk1-FLPo)10Sykr/J) mice for one generation. The resulting offspring were then genotyped to confirm removal of the neo/lacZ cassette and backcrossed to C57BL/6J mice for four generations

before being bred to homozygosity for the floxed BVRA allele. The floxed BVRA mice were crossed to mice expressing the Cre recombinase (B6.Cg-Tg(Alb-cre)21Mgn/J) specifically in the liver under the control of the albumin promoter (stock no. 003574; Jackson Labs, Bar Harbor ME) to create liver-specific BVRA knock-out mice (LBVRAKO). The studies were performed on 6-week-old male mice initially housed under standard conditions with full access to standard mouse chow and water. After this time, the mice were switched with full access to a 60% high fat diet (diet no. D12492; Research Diets, Inc., New Brunswick, NJ) for 12 weeks and allowed access to water.

**Body and Liver Composition**—Body composition changes were assessed at 4-week intervals throughout the study using magnetic resonance imaging (EchoMRI-900TM; Echo Medical System, Houston, TX). MRI measurements were performed in conscious mice placed in a thin-walled plastic cylinder with a cylindrical plastic insert added to limit movement of the mice.

## Hepatic BVRA Reduces Steatosis by Inhibition of GSK3 $\beta$

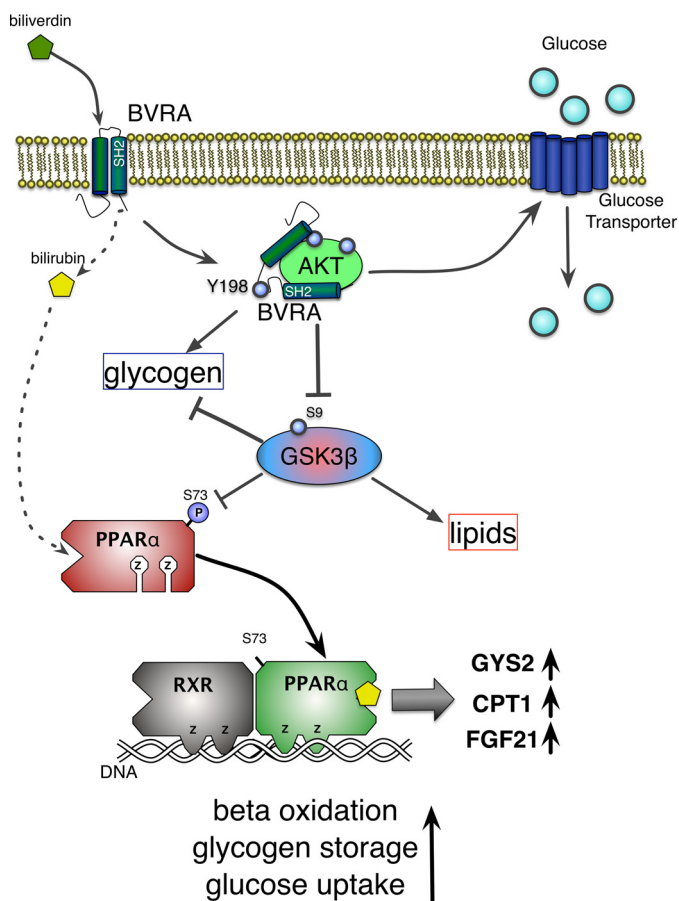


**FIGURE 8. Diagram of hepatic BVRA signaling to reduce fatty liver and increase glycogen storage.** BVRA reduces biliverdin to bilirubin, which binds to and activates the nuclear receptor PPAR $\alpha$  for the burning of fat by  $\beta$ -oxidation and storage of glycogen by increasing GYS2. Additionally, BVRA binds directly to AKT to increase phosphorylation, which inhibits GSK3 $\beta$  activity to increase glycogen and decrease lipid storage in the liver. The BVRA-AKT interaction also increases hepatic insulin sensitivity and glucose uptake.

The mice were briefly submitted to a low intensity electromagnetic field where fat mass, lean mass, free water, and total water were measured. At the end of the experimental protocol, the mice were euthanized by overdose of isoflurane anesthesia; the liver and fat were removed, and fat and lean mass were measured.

**Glucose and Insulin Tolerance Tests**—For GTTs, the mice were subjected to fasting (~8 h), and D-glucose (1 g/kg of body weight) was injected intraperitoneally. ITTs were conducted on fasted mice, and insulin (0.75 units/kg of body weight; Novolin human insulin) was injected intraperitoneally. Blood glucose was monitored at 0, 15, 30, 60, and 90 min after glucose or insulin injection.

**Liver Triglyceride Measurement**—Triglycerides were measured from 100 mg of liver tissue homogenized in 1 ml of 5% Nonidet P-40 in water. Homogenized tissues were then heated to 95 °C for 5 min and then centrifuged (13,000  $\times$  g) for 2 min. Tissue triglyceride levels were measured using a fluorometric assay kit according to the manufacturer's guidelines (PicoProbe triglyceride fluorometric assay kit; BioVision, Milpitas, CA). Tissue triglyceride levels were then normalized to the amount of starting tissues and expressed as mg of triglyceride/g of tissue weight. Samples from individual mice were run in duplicate and

averaged, and the averages of individual mice were then used to obtain group averages.

**Measurement of Hepatic Ser(P)<sup>9</sup> GSK3 $\beta$** —Hepatic levels of Ser(P)<sup>9</sup> GSK3 $\beta$  were measured using a specific Ser(P)<sup>9</sup> ELISA kit according to the manufacturer's guidelines (Ser(P)<sup>9</sup> GSK3 $\beta$  ELISA kit; Enzo, Farmingdale, NY). Briefly, 50 mg of liver tissue was homogenized in 500  $\mu$ l of RIPA buffer supplemented with phosphatase and protease inhibitors. Homogenates were then centrifuged briefly, and the supernatants were collected. ELISA was performed on diluted supernatants according to the manufacturer's protocols. Samples from individual mice were run in duplicate and averaged, and the averages of individual mice were then used to obtain group averages.

**Measurement of Plasma FGF21**—Plasma levels of FGF21 were measured from 50  $\mu$ l of plasma using a specific mouse/rat FGF21 ELISA (quantikine ELISA; R & D Systems, Minneapolis, MN) according to the manufacturer's instructions. The FGF21 ELISA was calibrated with a standard curve derived from a mouse/rat FGF21 standard provided by the manufacturer. FGF21 levels were measured in duplicate from individual mice, and FGF21 levels were determined by measurement at 450 nm on a plate reader. The concentrations are expressed as ng/ml.

**Immunofluorescence**—Immunofluorescence for BVRA was performed on paraformaldehyde-fixed liver samples. Sections of liver (20  $\mu$ m) were cut, rinsed in PBS, and blocked in 5% normal donkey serum for 1 h at 4 °C. The sections were then incubated with BVRA antibody in 5% normal donkey serum overnight at 4 °C and then rinsed in PBS. BVRA was detected using a rabbit anti-BVRA antibody (ADI-OSA-450, 1:100; Enzo Life Sciences, Farmingdale, NY). Antibody labeling was visualized using a fluorescence-labeled donkey anti-rabbit Alexa 488 (A-21206, 1:1000; Invitrogen) secondary antibody. Following a final rinse in PBS and DAPI counterstaining, the samples were covered with Fluoromount-G mounting medium (Southern Biotech, Birmingham, AL) and coverslipped before imaging. All samples were examined using a Leica TCS SP5 laser scanning confocal microscope (Leica Microsystems, Buffalo Grove, IL).

**Liver Oil Red O Staining**—To determine the effects of treatment on hepatic lipid accumulation, the livers were mounted and frozen in Tissue-Tek O.C.T and sectioned at 10  $\mu$ m. Frozen sections were air-dried and fixed in 10% neutral buffered formalin. The sections were briefly rinsed in tap water followed by 60% isopropanol and stained for 15 min in Oil Red O solution. The sections were further rinsed in 60% isopropanol, and the nuclei were stained with hematoxylin followed by aqueous mounting and coverslipping. The degree of Oil Red O staining was determined at 40 $\times$  magnification using a color Axiocam 105 camera with Zen 2 software attached to a Zeiss Axioplan microscope. The images were analyzed using National Institutes of Health ImageJ software, and to ensure accuracy of measurement, six images of each animal were analyzed and averaged into a single measurement. The measurements were obtained from three individual animals/group. The data are presented as the averages  $\pm$  S.E. of the percentage of Oil Red O staining for each group.

**Periodic Acid Schiff Staining for Glycogen**—Formalin-fixed, paraffin-embedded liver sections were cut at 5  $\mu$ m and deparaffinized, followed by hydration. The sections were oxidized in



0.5% periodic acid solution for 5 min, rinsed in distilled water, and stained in Schiff's reagent for 15 min. The sections were washed in tap water, and the nuclei were counterstained with hematoxylin, rinsed, dehydrated, and coverslipped with Eukitt (Electron Microscopy Sciences, Hatfield, PA). For analysis, two or three random fields/slide were taken from three liver samples from each group at magnification of 40 $\times$  on a Zeiss Axioplan microscope equipped with an Axiocam 105 color camera and Zen 2 software.

**Fasting Glucose and Insulin**—Following an overnight fast, a blood sample was obtained via orbital sinus under isoflurane anesthesia. Blood glucose was measured using an Accu-Chek Advantage glucometer (Roche Applied Science). Fasting plasma insulin concentrations were determined by ELISA (Linco Insulin ELISA kit) as previously described (48).

**Biliverdin Reductase Assay**—Biliverdin reductase activity was measured using a modified assay (49). Samples were homogenized in a potassium phosphate buffer (10 mM potassium phosphate, 25 mM sucrose, 1 mM EDTA, and 0.1 mM PMSF). Biliverdin reductase activity was then measured in 0.5 mg of protein homogenate in an assay buffer (50 mM Tris-base, 1 mM EDTA, pH 8.7, 1.2 mM NADPH, and 0.03 mM biliverdin). The activity assay was done in a final volume of 1 ml. The reactions were incubated in the dark for 15 min at 37 °C following by a 5-min incubation in the dark at 95 °C. Bilirubin levels in the assay samples were determined by spectroscopy at 468 nm using a standard curve of bilirubin IX $\alpha$  (50–300  $\mu$ M). BVR activity was expressed as  $\mu$ mol of bilirubin/min/mg of protein.

**Promoter Reporter Assays and PPAR $\alpha$  Mutants Construct Generation**—The Cos7 green kidney monkey cells used for the promoter assays were routinely cultured and maintained in DMEM containing 10% bovine calf serum or FBS with 1% penicillin-streptomycin. Expression vector for PPAR $\alpha$ -3X-FLAG CMV was constructed as previously described (13). The S73A and S73D PPAR $\alpha$  mutants were generated using QuikChange site-directed mutagenesis kit with the PPAR $\alpha$ -3X-FLAG CMV plasmid according to the manufacturer's protocol (Stratagene, La Jolla, CA). The HA-tagged GSK3 $\beta$  WT and K85A pcDNA3 was a gift from Jim Woodgett (Addgene plasmids 14753 and 14755, respectively) (12). PPAR $\alpha$  minimal promoter PPRE-3tk-luciferase activity was measured by luciferase in the previous of PPAR $\alpha$  and/or GSK3 $\beta$ , and pRL-CMV *Renilla* reporter for normalization to transfection efficiency. Transient transfection was achieved using GeneFect (Alkali Scientific, Inc.). 24-h post-transfected cells were treated for 24 h in dialyzed fatty acid free FBS and then lysed. The luciferase assay was performed using the Promega dual luciferase assay system (Promega, Madison, WI).

**Quantitative Real Time PCR Analysis**—Total RNA was harvested from WT and BVRA knock-out mice by lysing livers using a Qiagen Tissue Lyser LT (Qiagen) and then extraction by 5-Prime PerfectPure RNA tissue kit (Fisher Scientific). Total RNA was read on a NanoDrop 2000 spectrophotometer (Thermo Fisher Scientific), and cDNA was synthesized using a high capacity cDNA reverse transcription kit (Applied Biosystems). PCR amplification of the cDNA was performed by quantitative real time PCR using TrueAmp SYBR Green qPCR SuperMix (Alkali Scientific). The thermocycling protocol con-

sisted of 5 min at 95 °C, 40 cycles of 15 s at 95 °C, and 30 s at 60 °C and finished with a melting curve ranging from 60 to 95 °C to allow distinction of specific products. Normalization was performed in separate reactions with primers to GAPDH mRNA.

**Gel Electrophoresis and Western Blotting**—Mouse tissues were flash frozen in liquid nitrogen during harvesting and stored at –80 °C. For gel electrophoresis, 50–100 mg of cut tissue was then resuspended in 3 volumes of CellLytic Buffer (Sigma C3228) plus 10% protease inhibitor mixture (P2714-1BTL; Sigma) and Halt phosphatase inhibitor mixture (PI78420; Fisher), then incubated on ice for 30 min followed by lysing the livers using a Qiagen Tissue Lyser LT (Qiagen), and then centrifuged at 100,000  $\times$  *g* at 4 °C. Protein samples were resolved by SDS-polyacrylamide gel electrophoresis and electrophoretically transferred to Immobilon-FL membranes. The membranes were blocked at room temperature for 2 h in TBS (10 mM Tris-HCl, pH 7.4, and 150 mM NaCl) containing 3% BSA. Subsequently, the membranes were incubated overnight at 4 °C with the following antibodies: PPAR $\alpha$  (sc-9000; Santa Cruz Biotechnology, Santa Cruz, CA), heat shock protein 90 (HSP90) (13119; Santa Cruz), serine 73 phospho-PPAR $\alpha$  (described below), insulin receptor  $\beta$  (sc-711; Santa Cruz), GYS2 (sc-47109; Santa Cruz), GYS phosphoserine 641 (3891; Cell Signaling), AKT (9272S; Cell Signaling), phospho-AKT (4060S; Cell Signaling), AMPK (2532S; Cell Signaling), phospho-AMPK (2535S; Cell Signaling), FAS (3180S; Cell Signaling), phospho-ACC (3661S; Cell Signaling), GSK3 $\beta$  (9832S; Cell Signaling), phospho-GSK3 $\beta$  (9336S; Cell Signaling), and CPT1A (ab128568; Abcam). After three washes in TBS + 0.1% Tween 20, the membrane was incubated with an infrared anti-rabbit (IRDye 800, *green*) or anti-mouse (IRDye 680, *red*) secondary antibody labeled with IRDye infrared dye (LI-COR Biosciences) (1:10,000 dilution in TBS) for 2 h at 4 °C. Immunoreactivity was visualized and quantified by infrared scanning in the Odyssey system (LI-COR Biosciences).

**Generation of Serine 73 Phospho-PPAR $\alpha$  Antibody**—To generate a phosphospecific antibody to a peptide corresponding to serine 73 at the N terminus of PPAR $\alpha$ , 15 amino acids with phosphorylated serine 73 (VITDTLpSPASSPSS-Cys) was synthesized and purified by Pacific Immunology (Ramona, CA). The Ser(P)<sup>73</sup>-PPAR $\alpha$  antibody was made as previously described in Ref. 13. In brief, an N-terminal cysteine was added to the peptide as a linker, followed by conjugation to a peptide carrier protein keyhole limpet hemocyanin and adjuvant-based immunization in a female New Zealand White rabbit. Preimmune serum was collected before injecting the rabbits with Ser(P)<sup>73</sup>-PPAR $\alpha$  peptide conjugate. The rabbits were boosted 2 weeks after injection with the Ser(P)<sup>73</sup>-PPAR $\alpha$  peptide with complete Freund's adjuvant and subsequently boosted two more times with incomplete Freund's adjuvant every 2 weeks. Serum was collected at 2 months and analyzed via ELISA for Ser(P)<sup>73</sup>-PPAR $\alpha$  specific antibodies. Serum of high titer was obtained and subjected to one round of affinity purification using the Ser(P)<sup>73</sup>-PPAR $\alpha$  peptide.

**In Vitro Kinase Assay**—PPAR $\alpha$ , PPAR $\alpha$  mutants, and PPAR $\alpha$  domains were expressed as maltose-binding protein (MBP) fusion protein in DH5 $\alpha$  bacteria and purified using amylose



## Hepatic BVRA Reduces Steatosis by Inhibition of GSK3 $\beta$

resin (New England Biolabs) as described previously (16). pMAL rPPAR $\alpha$  mutants were generated using a QuikChange site-directed mutagenesis kit according to the manufacturer's protocol (Stratagene). Phosphorylation of MPB-PPAR $\alpha$ , MBP-PPAR $\alpha$  domains, and MPB-PPAR $\alpha$  mutants was performed by incubating 2  $\mu$ g of MBP-PPAR $\alpha$ , 5 or 25 ng of active GSK3 $\beta$  (Upstate Biotechnology, Lake Placid, NY), and 1  $\mu$ Ci of [ $\gamma$ -<sup>32</sup>P]ATP (PerkinElmer Life Sciences) in kinase reaction buffer (40 mM MOPS, pH 7.0, 1 mM EDTA) according to the manufacturer's protocol for 90 min at 30 °C. The proteins were heated to 95 °C for 3 min and were separated on an 8% Tris-glycine gel, dried, and visualized by autoradiography ( $n = 3$  separate experiments).

**Ubiquitination of PPAR $\alpha$** —After transfection (V5-rPPAR $\alpha$ , HA-ubiquitin, pcDNA3.1 GSK3 $\beta$ , V5-rPPAR $\alpha$  S73A, or empty vector; plasmids are described below) recovery, Cos-1 cells were co-treated with 50  $\mu$ M WY-14643 ([4-chloro-6-(2,3-zylin-dino)-2-pyrimidinylthio] acetic acid, CAS no. 50892-23-4; BIOMOL International, Plymouth Meeting, PA) or 0.1% DMSO in the presence of 5  $\mu$ M MG132 (carbobenzoxy-L-leucyl-L-leucyl-L-leucinal Z-LLL-CHO; Calbiochem, San Diego, CA) for 4 h. The cells were lysed in 1 ml of RIPA buffer supplemented with mammalian protease inhibitor mixture and 10  $\mu$ g/ml  $\alpha$ -iodoacetamide (Calbiochem) on ice for 20 min. Equal amounts of protein (1.5 mg) were precleared with 50  $\mu$ l of protein G-Sepharose for 2 h before incubation with 75  $\mu$ l of protein G-Sepharose (Santa Cruz Biotechnology, Santa Cruz, CA) plus 1  $\mu$ l anti-V5 antibody (R960-25, 1:5000; Invitrogen) overnight at 4 °C with rocking. Immune complexes were washed four times with RIPA buffer plus 10  $\mu$ g/ml  $\alpha$ -iodoacetamide, and proteins were eluted from the resin with 2 $\times$  Tricine sample buffer, heated at 80 °C for 5 min, and separated on an 8% Tricine gel. The proteins were transferred to Hybond-ECL nitrocellulose, and the membrane was boiled in water for 5 min, immediately put into 5% nonfat dry milk blocking buffer, and probed for ubiquitinated PPAR $\alpha$  using V5-HRP antibody (R96125, 1:5000; Invitrogen) for detection of mono-ubiquitination and HA-antibody (SC-7392, 1:1000; Santa Cruz Biotechnology) for detection of polyubiquitination via Western blotting with detection by the addition of [<sup>125</sup>I]streptavidin (1:10,000; GE Healthcare) with  $n = 3$  separate experiments. Plasmids for PPAR $\alpha$  ubiquitination analysis are as follows: pcDNA3.1/V5-His-rPPAR $\alpha$  (V5-rPPAR $\alpha$ ) was described previously (16), V5-rPPAR $\alpha$  S73A mutant was generated using a QuikChange site-directed mutagenesis kit according to the manufacturer's protocol (Stratagene), pcDNA3.1 GSK3 $\beta$  was from Curtis Omiecinski (Pennsylvania State University, University Park, PA), and HA-ubiquitin was from Dirk Bohmann (University of Rochester, Rochester, NY).

**Statistical Analysis**—The data were analyzed with Prism 6 (GraphPad Software) using analysis of variance combined with Tukey's post-test to compare pairs of group means or unpaired  $t$  tests. The results are expressed as means  $\pm$  S.E. Additionally, one-way analysis of variance with a least significant difference post hoc test was used to compare mean values between multiple groups, and a two-tailed, and a two-way analysis of variance was utilized in multiple comparisons, followed by the Bonfer-

roni post hoc analysis to identify interactions.  $p$  values of 0.05 or smaller were considered statistically significant.

**Author Contributions**—T. D. H. and D. E. S. conceived and coordinated the study and wrote the paper. K. A. B. and J. P. V. H. designed, performed, and analyzed the experiments shown in Fig. 6 (A–D) and contributed to the preparation of the figures and manuscript. T. D. H., L. M., and A. N.-K. designed, performed, and analyzed the experiments shown in Figs. 2 (A and B), 3 (D–F), 4, 5 (A–C), 6 (E and F), and 7 and contributed to the preparation of the figures. T. D. H. had the Ser(P)<sup>73</sup> PPAR $\alpha$ -Ab generated and tested specificity. Additionally, A. N.-K. performed the imaging in Figs. 3B, 4B, and 7 (B and C). D. E. S. developed the liver-specific biliverdin reductase knockout mice. D. E. S., H. A. D., A. A. A., and M. W. H. developed and analyzed the experiments shown in Figs. 1, 2 (C and D), 3 (A–C), 4A, and 5D and contributed to the preparation of the figures. All authors reviewed the results and approved the final version of the manuscript.

## References

1. John, K., Marino, J. S., Sanchez, E. R., and Hinds, T. D., Jr. (2016) The glucocorticoid receptor: cause or cure for obesity? *Am. J. Physiol. Endocrinol. Metab.* **310**, E249–E257
2. Day, C. P., and James, O. F. (1998) Steatohepatitis: a tale of two "hits"? *Gastroenterology* **114**, 842–845
3. Tilg, H., and Moschen, A. R. (2010) Evolution of inflammation in non-alcoholic fatty liver disease: the multiple parallel hits hypothesis. *Hepatology* **52**, 1836–1846
4. Hinds, T. D., Jr., Sodhi, K., Meadows, C., Fedorova, L., Puri, N., Kim, D. H., Peterson, S. J., Shapiro, J., Abraham, N. G., and Kappas, A. (2013) Increased HO-1 levels ameliorate fatty liver development through a reduction of heme and recruitment of FGF21. *Obesity (Silver Spring)* **22**, 705–712
5. O'Brien, L., Hosick, P. A., John, K., Stec, D. E., and Hinds, T. D., Jr. (2015) Biliverdin reductase isozymes in metabolism. *Trends Endocrinol. Metabol.* **26**, 212–220
6. Pereira, P. J., Macedo-Ribeiro, S., Párraga, A., Pérez-Luque, R., Cunningham, O., Darcy, K., Mantle, T. J., and Coll, M. (2001) Structure of human biliverdin IX $\beta$  reductase, an early fetal bilirubin IX $\beta$  producing enzyme. *Nat. Struct. Biol.* **8**, 215–220
7. Lerner-Marmarosh, N., Shen, J., Torno, M. D., Kravets, A., Hu, Z., and Maines, M. D. (2005) Human biliverdin reductase: a member of the insulin receptor substrate family with serine/threonine/tyrosine kinase activity. *Proc. Natl. Acad. Sci. U.S.A.* **102**, 7109–7114
8. Stec, D. E., John, K., Trabbic, C. J., Luniwal, A., Hankins, M. W., Baum, J., and Hinds, T. D. (2016) Bilirubin binding to PPAR $\alpha$  inhibits lipid accumulation. *PLoS One* **11**, e0153427
9. Lu, K., Han, M., Ting, H. L., Liu, Z., and Zhang, D. (2013) Scutellarin from *Scutellaria baicalensis* suppresses adipogenesis by upregulating PPAR $\alpha$  in 3T3-L1 cells. *J. Nat. Prod.* **76**, 672–678
10. Goto, T., Lee, J. Y., Teraminami, A., Kim, Y. I., Hirai, S., Uemura, T., Inoue, H., Takahashi, N., and Kawada, T. (2011) Activation of peroxisome proliferator-activated receptor- $\alpha$  stimulates both differentiation and fatty acid oxidation in adipocytes. *J. Lipid Res.* **52**, 873–884
11. Liu, J., Wang, L., Tian, X. Y., Liu, L., Wong, W. T., Zhang, Y., Han, Q. B., Ho, H. M., Wang, N., Wong, S. L., Chen, Z. Y., Yu, J., Ng, C. F., Yao, X., and Huang, Y. (2015) Unconjugated bilirubin mediates heme oxygenase-1-induced vascular benefits in diabetic mice. *Diabetes* **64**, 1564–1575
12. Stambolic, V., and Woodgett, J. R. (1994) Mitogen inactivation of glycogen synthase kinase-3 $\beta$  in intact cells via serine 9 phosphorylation. *Biochem. J.* **303**, 701–704
13. Hinds, T. D., Jr., Ramakrishnan, S., Cash, H. A., Stechsulte, L. A., Heinrich, G., Najjar, S. M., and Sanchez, E. R. (2010) Discovery of glucocorticoid receptor- $\beta$  in mice with a role in metabolism. *Mol. Endocrinol.* **24**, 1715–1727

14. Stienstra, R., Mandard, S., Patsouris, D., Maass, C., Kersten, S., and Müller, M. (2007) Peroxisome proliferator-activated receptor  $\alpha$  protects against obesity-induced hepatic inflammation. *Endocrinology* **148**, 2753–2763
15. Lebrun, V., Molendi-Coste, O., Lanthier, N., Sempoux, C., Cani, P. D., van Rooijen, N., Stärkel, P., Horsmans, Y., and Leclercq, I. A. (2013) Impact of PPAR- $\alpha$  induction on glucose homeostasis in alcohol-fed mice. *Clin. Sci.* **125**, 501–511
16. Harano, Y., Yasui, K., Toyama, T., Nakajima, T., Mitsuyoshi, H., Mimani, M., Hirasawa, T., Itoh, Y., and Okanoue, T. (2006) Fenofibrate, a peroxisome proliferator-activated receptor  $\alpha$  agonist, reduces hepatic steatosis and lipid peroxidation in fatty liver Shionogi mice with hereditary fatty liver. *Liver Int.* **26**, 613–620
17. Burns, K. A., and Vanden Heuvel, J. P. (2007) Modulation of PPAR activity via phosphorylation. *Biochim. Biophys. Acta* **1771**, 952–960
18. Adams, M., Reginato, M. J., Shao, D., Lazar, M. A., and Chatterjee, V. K. (1997) Transcriptional activation by peroxisome proliferator-activated receptor  $\gamma$  is inhibited by phosphorylation at a consensus mitogen-activated protein kinase site. *J. Biol. Chem.* **272**, 5128–5132
19. Hinds, T. D., Jr., Stechschulte, L. A., Cash, H. A., Whisler, D., Banerjee, A., Yong, W., Khuder, S. S., Kaw, M. K., Shou, W., Najjar, S. M., and Sanchez, E. R. (2011) Protein phosphatase 5 mediates lipid metabolism through reciprocal control of glucocorticoid receptor and peroxisome proliferator-activated receptor- $\gamma$  (PPAR $\gamma$ ). *J. Biol. Chem.* **286**, 42911–42922
20. Schädinger, S. E., Bucher, N. L., Schreiber, B. M., and Farmer, S. R. (2005) PPAR $\gamma$ 2 regulates lipogenesis and lipid accumulation in steatotic hepatocytes. *Am. J. Physiol. Endocrinol. Metab.* **288**, E1195–E1205
21. Imazu, M., Strickland, W. G., Chrisman, T. D., and Exton, J. H. (1984) Phosphorylation and inactivation of liver glycogen synthase by liver protein kinases. *J. Biol. Chem.* **259**, 1813–1821
22. Oreña, S. J., Torchia, A. J., and Garofalo, R. S. (2000) Inhibition of glycogen-synthase kinase 3 stimulates glycogen synthase and glucose transport by distinct mechanisms in 3T3-L1 adipocytes. *J. Biol. Chem.* **275**, 15765–15772
23. Ibrahim, S. H., Akazawa, Y., Cazanave, S. C., Bronk, S. F., Elmi, N. A., Werneburg, N. W., Billadeau, D. D., and Gores, G. J. (2011) Glycogen synthase kinase-3 (GSK-3) inhibition attenuates hepatocyte lipopoptosis. *J. Hepatol.* **54**, 765–772
24. Chang, Y. S., Tsai, C. T., Huangfu, C. A., Huang, W. Y., Lei, H. Y., Lin, C. F., Su, I. J., Chang, W. T., Wu, P. H., Chen, Y. T., Hung, J. H., Young, K. C., and Lai, M. D. (2011) ACSL3 and GSK-3 $\beta$  are essential for lipid upregulation induced by endoplasmic reticulum stress in liver cells. *J. Cell. Biochem.* **112**, 881–893
25. Gibbs, P. E., Lerner-Marmarosh, N., Poulin, A., Farah, E., and Maines, M. D. (2014) Human biliverdin reductase-based peptides activate and inhibit glucose uptake through direct interaction with the kinase domain of insulin receptor. *FASEB J.* **28**, 2478–2491
26. Lerner-Marmarosh, N., Miralem, T., Gibbs, P. E., and Maines, M. D. (2008) Human biliverdin reductase is an ERK activator; hBVR is an ERK nuclear transporter and is required for MAPK signaling. *Proc. Natl. Acad. Sci. U.S.A.* **105**, 6870–6875
27. Murgia, M., Jensen, T. E., Cusinato, M., Garcia, M., Richter, E. A., and Schiaffino, S. (2009) Multiple signalling pathways redundantly control glucose transporter GLUT4 gene transcription in skeletal muscle. *J. Physiol.* **587**, 4319–4327
28. Habets, D. D., Coumans, W. A., El Hasnaoui, M., Zarrinashneh, E., Bertrand, L., Viollet, B., Kiens, B., Jensen, T. E., Richter, E. A., Bonen, A., Glatz, J. F., and Luiken, J. J. (2009) Crucial role for LKB1 to AMPK $\alpha$ 2 axis in the regulation of CD36-mediated long-chain fatty acid uptake into cardiomyocytes. *Biochim. Biophys. Acta* **1791**, 212–219
29. Chavez, J. A., Roach, W. G., Keller, S. R., Lane, W. S., and Lienhard, G. E. (2008) Inhibition of GLUT4 translocation by Tbc1d1, a Rab GTPase-activating protein abundant in skeletal muscle, is partially relieved by AMP-activated protein kinase activation. *J. Biol. Chem.* **283**, 9187–9195
30. Mandard, S., Stienstra, R., Escher, P., Tan, N. S., Kim, I., Gonzalez, F. J., Wahli, W., Desvergne, B., Müller, M., and Kersten, S. (2007) Glycogen synthase 2 is a novel target gene of peroxisome proliferator-activated receptors. *Cell. Mol. Life Sci.* **64**, 1145–1157
31. Zeng, R., Yao, Y., Han, M., Zhao, X., Liu, X. C., Wei, J., Luo, Y., Zhang, J., Zhou, J., Wang, S., Ma, D., and Xu, G. (2008) Biliverdin reductase mediates hypoxia-induced EMT via PI3-kinase and Akt. *J. Am. Soc. Nephrol.* **19**, 380–387
32. Pachori, A. S., Smith, A., McDonald, P., Zhang, L., Dzau, V. J., and Melo, L. G. (2007) Heme-oxygenase-1-induced protection against hypoxia/reoxygenation is dependent on biliverdin reductase and its interaction with PI3K/Akt pathway. *J. Mol. Cell. Cardiol.* **43**, 580–592
33. Badman, M. K., Pissios, P., Kennedy, A. R., Koukos, G., Flier, J. S., and Maratos-Flier, E. (2007) Hepatic fibroblast growth factor 21 is regulated by PPAR $\alpha$  and is a key mediator of hepatic lipid metabolism in ketotic states. *Cell Metab.* **5**, 426–437
34. Berglund, E. D., Li, C. Y., Bina, H. A., Lynes, S. E., Michael, M. D., Shanafelt, A. B., Kharitononkov, A., and Wasserman, D. H. (2009) Fibroblast growth factor 21 controls glycemia via regulation of hepatic glucose flux and insulin sensitivity. *Endocrinology* **150**, 4084–4093
35. Chau, M. D., Gao, J., Yang, Q., Wu, Z., and Gromada, J. (2010) Fibroblast growth factor 21 regulates energy metabolism by activating the AMPK-SIRT1-PGC-1 $\alpha$  pathway. *Proc. Natl. Acad. Sci. U.S.A.* **107**, 12553–12558
36. Lundäsen, T., Hunt, M. C., Nilsson, L. M., Sanyal, S., Angelin, B., Alexson, S. E., and Rudling, M. (2007) PPAR $\alpha$  is a key regulator of hepatic FGF21. *Biochem. Biophys. Res. Commun.* **360**, 437–440
37. Miralem, T., Lerner-Marmarosh, N., Gibbs, P. E., Jenkins, J. L., Heimiller, C., and Maines, M. D. (2016) Interaction of human biliverdin reductase with Akt/protein kinase B and phosphatidylinositol-dependent kinase 1 regulates glycogen synthase kinase 3 activity: a novel mechanism of Akt activation. *FASEB J.* **30**, 2926–2944
38. Banko, N. S., McAlpine, C. S., Venegas-Pino, D. E., Raja, P., Shi, Y., Khan, M. I., and Werstuck, G. H. (2014) Glycogen synthase kinase 3 $\alpha$  deficiency attenuates atherosclerosis and hepatic steatosis in high fat diet-fed low density lipoprotein receptor-deficient mice. *Am. J. Pathol.* **184**, 3394–3404
39. Bowes, A. J., Khan, M. I., Shi, Y., Robertson, L., and Werstuck, G. H. (2009) Valproate attenuates accelerated atherosclerosis in hyperglycemic apoE-deficient mice: evidence in support of a role for endoplasmic reticulum stress and glycogen synthase kinase-3 in lesion development and hepatic steatosis. *Am. J. Pathol.* **174**, 330–342
40. Lee, S., Yang, W. K., Song, J. H., Ra, Y. M., Jeong, J. H., Choe, W., Kang, I., Kim, S. S., and Ha, J. (2013) Anti-obesity effects of 3-hydroxychromone derivative, a novel small-molecule inhibitor of glycogen synthase kinase-3. *Biochem. Pharmacol.* **85**, 965–976
41. Yang, Y., Li, W., Liu, Y., Li, Y., Gao, L., and Zhao, J. J. (2014)  $\alpha$ -lipoic acid attenuates insulin resistance and improves glucose metabolism in high fat diet-fed mice. *Acta Pharmacol. Sin.* **35**, 1285–1292
42. Fang, X., Yu, S. X., Lu, Y., Bast, R. C., Jr., Woodgett, J. R., and Mills, G. B. (2000) Phosphorylation and inactivation of glycogen synthase kinase 3 by protein kinase A. *Proc. Natl. Acad. Sci. U.S.A.* **97**, 11960–11965
43. Stocker, R., Yamamoto, Y., McDonagh, A. F., Glazer, A. N., and Ames, B. N. (1987) Bilirubin is an antioxidant of possible physiological importance. *Science* **235**, 1043–1046
44. Stocker, R. (2004) Antioxidant activities of bile pigments. *Antioxid. Redox. Signal.* **6**, 841–849
45. Jang, B. K. (2012) Elevated serum bilirubin levels are inversely associated with nonalcoholic fatty liver disease. *Clin. Mol. Hepatol.* **18**, 357–359
46. Kwak, M. S., Kim, D., Chung, G. E., Kang, S. J., Park, M. J., Kim, Y. J., Yoon, J. H., and Lee, H. S. (2012) Serum bilirubin levels are inversely associated with nonalcoholic fatty liver disease. *Clin. Mol. Hepatol.* **18**, 383–390
47. Puri, K., Nobili, V., Melville, K., Corte, C. D., Sartorelli, M. R., Lopez, R., Feldstein, A. E., and Alkhoury, N. (2013) Serum bilirubin level is inversely associated with nonalcoholic steatohepatitis in children. *J. Pediatr. Gastroenterol. Nutr.* **57**, 114–118
48. Csongradi, E., Docarmo, J. M., Dubinion, J. H., Vera, T., and Stec, D. E. (2012) Chronic HO-1 induction with cobalt protoporphyrin (CoPP) treatment increases oxygen consumption, activity, heat production and lowers body weight in obese melanocortin-4 receptor-deficient mice. *Int. J. Obes. (Lond.)* **36**, 244–253
49. Huang, T. J. (2002) Detection of biliverdin reductase activity. *Curr. Protoc. Toxicol.* **9**, 4.1–4.10